Decay of the $N = 126$, ^{213}Fr nucleus

Pragati,[1] A. Y. Deo,[1,*] Zs. Podolyák,[2] P. M. Walker,[2,†] A. Algora,[3,‡] B. Rubio,[3] J. Agramunt,[3] L. M. Fraile,[4] N. Al-Dahan,[2,§]
N. Alkhomashi,[2,‖] J. A. Briz,[5] M. E. Estevez Aguado,[3] G. Farrelly,[2] W. Gelletly,[2,3] A. Herlert,[6,¶] U. Köster,[7] and A. Maira[5,#]

[1]*Department of Physics, Indian Institute of Technology Roorkee, Roorkee 247667, India*
[2]*Department of Physics, University of Surrey, Guildford GU2 7XH, United Kingdom*
[3]*IFIC, CSIC - Universidad de Valencia, E-46071 Valencia, Spain*
[4]*Grupo de Física Nuclear, Facultad de Físicas, Universidad Complutense, E-28040 Madrid, Spain*
[5]*Instituto de Estructura de la Materia, CSIC, E-28006 Madrid, Spain*
[6]*ISOLDE, PH Department, CERN, CH-1211 Geneva 23, Switzerland*
[7]*Institut Laue-Langevin, 71 Avenue des Martyrs, 38042 Grenoble Cedex 9, France*
(Received 28 September 2016; published 14 December 2016)

γ rays following the EC/β^+ and α decay of the $N = 126$, ^{213}Fr nucleus have been observed at the CERN isotope separator on-line (ISOLDE) facility with the help of γ-ray and conversion-electron spectroscopy. These γ rays establish several hitherto unknown excited states in ^{213}Rn. Also, five new α-decay branches from the ^{213}Fr ground state have been discovered. Shell model calculations have been performed to understand the newly observed states in ^{213}Rn.

I. INTRODUCTION

The structure of nuclei in the proximity of shell closures is a topic of great interest because it gives direct information on the underlying shell-model orbitals. This information is of particular importance to test the accuracy of shell-model predictions and for further improvements to the model, if required. Apart from this, a precise knowledge of α decays in the $N = 126$ closed-shell region is important for understanding the nuclear structure around the next neutron shell closure beyond $N = 126$ [1,2].

The single-particle structure around $Z = 90$ and $N = 126$ is governed by proton—$1h_{9/2}$, $1i_{13/2}$ and neutron—$2f_{5/2}$, $3p_{1/2}$, $2g_{9/2}$, and $1i_{11/2}$ shell model orbitals. The states with dominant single-particle configurations, especially those with low-j, are often established by observing γ rays following the decay of the parent nucleus. However, no such γ rays were known in ^{213}Rn prior to our study. In addition, among the

---

*aydeofph@iitr.ac.in

†Also at ISOLDE, PH Department, CERN, CH-1211 Geneva 23, Switzerland.

‡Also at Institute of Nuclear Research of the Hungarian Academy of Sciences, Debrecen H-4001, Hungary.

§Present address: Department of Physics, University of Kerbala, Kerbala, Iraq.

‖Present address: KACST, P.O. Box 6086, Riyadh 11442, Saudi Arabia.

¶Present address: FAIR GmbH, Planckstrasse 1, D-64291 Darmstadt, Germany.

#Present address: CMAM, Universidad Autónoma de Madrid, E-28049, Madrid, Spain.

$N = 126$ isotones, only ^{211}At has a substantial EC/β^+-decay branching ratio (58.2%) [3], while all the other isotones are known to decay with less than 1% β-decay branch [4–12]. Nevertheless, we were able to identify γ rays in ^{213}Rn populated in the EC/β^+ decay of ^{213}Fr with a decay branch of only 0.56% [13]. It is also interesting to note that very little experimental information is available on the unique positive-parity $\pi 1i_{13/2}$ orbitals in this region.

Furthermore, α-decay studies not only play a major role in discoveries of superheavy elements [14,15] but also provide crucial information on the decay of closed-shell nuclei near the proton drip line [16,17]. The experimental values of α-decay half-lives and branching ratios are useful in establishing the decay chain of superheavy nuclei. It is, therefore, essential to have a proper theoretical understanding of α decay in the $N = 126$ region [1,2], which will further aid in research on superheavy nuclei, and detailed experimental data on α decay in the $N = 126$ region is desired.

^{213}Fr can be used to study the influence of electron screening on the α-decay half-life [18]. It also serves as a reference isotope for precision laser spectroscopy studies of the Bohr-Weisskopf effect in francium isotopes [19]. Furthermore, ^{209}At is proposed as an alternative isotope to ^{211}At for medical imaging due to its favorable x-ray and γ-ray intensities [20]. The proposed route of ^{209}At production involves the α decay of ^{213}Fr.

In this paper, we present the first EC/β^+-decay study of the $N = 126$, ^{213}Fr nucleus, which establishes several new levels in the daughter nucleus. Also, the data reveal five new α-decay branches of ^{213}Fr.

II. EXPERIMENTAL SETUP

The experiment was performed at the CERN isotope separator on-line (ISOLDE) facility, where a 1.4-GeV proton beam from the CERN PS-Booster impinged on a 46 g/cm^2 UC$_x$ target. Pulses of 3×10^{13} protons, in a regular interval of

FIG. 1. Transmission efficiency curve of the MINI-ORANGE spectrometer.

FIG. 2. Part of the singles conversion-electron spectrum, illustrating transitions from excited states in ^{213}Fr, ^{213}Rn, ^{209}At, and ^{209}Po with the $A = 213$ GPS setting. The transitions are labeled with the corresponding γ-ray energies.

5.6 s, hit the target of ISOLDE. The spallation products diffused out of the target that was at $2100\,^\circ$C to a $2100\,^\circ$C hot tungsten transfer tube, where francium atoms were surface ionized. The ionized atoms were accelerated to 30 keV and then separated in mass by the ISOLDE general purpose separator (GPS). The surface ionization potentials of the $A = 213$ isobars are significantly higher (>7.2 eV) than those for francium (4.07 eV) and radium (5.28 eV), resulting in orders-of-magnitude lower surface ionization efficiency and, hence, a quite pure beam of francium with a weak admixture of radium [21]. The mass-separated $A = 213$ beam was collected on a tape and transported to a measurement station at regular intervals of 33.6 s. An electron detection system and two high-purity germanium (HPGe) detectors were used for internal-conversion-electron and γ-ray studies, respectively. A Si(Li) detector with a thickness of 4 mm, an active area of 300 mm^2, and an energy resolution of 2.0 keV at $\sim$500 keV was used in conjunction with a MINI-ORANGE spectrometer [22,23] to form the electron detection system. The MINI-ORANGE spectrometer is composed of a set of six equally spaced permanent magnets. The distance between the MINI-ORANGE spectrometer and the detector was chosen to be 110 mm to maximize the electron transmission efficiency in the energy range of 400–800 keV. Figure 1 shows the transmission efficiency curve of the MINI-ORANGE spectrometer that was obtained using decays with well-defined multipolarities of different reference nuclides studied in the same experiment. Figure 2 shows part of the conversion-electron spectrum for $A = 213$ products.

The two HPGe detectors had absolute efficiencies between $\sim$4% and $\sim$0.3% and a resolution of 1.0 and 2.0 keV at $\sim$100 keV and $\sim$1.5 MeV, respectively. The details of the experimental setup can be found elsewhere [23]. The energy and efficiency calibrations of the HPGe detectors were obtained using standard ^{133}Ba and ^{152}Eu sources.

The five-parameter event data were acquired using a triggerless digital data acquisition system Pixie4 [24]. The signals from the motion of the magnetic tape, preamplifiers
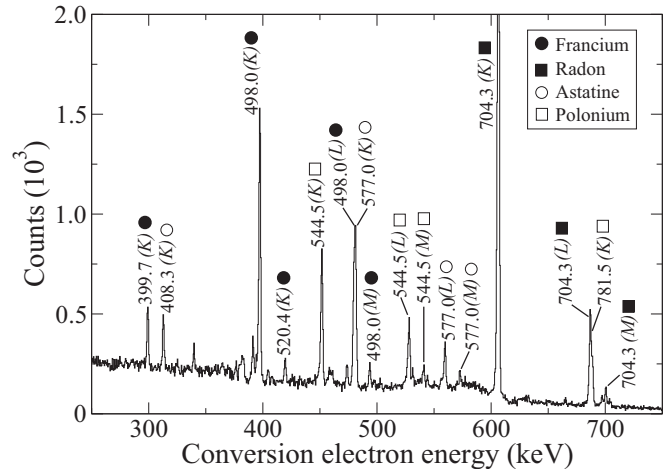
of the two HPGe detectors and the Si(Li) detectors, and the proton pulse were digitized and time stamped. The data from the HPGe detectors and the Si(Li) detectors were sorted into various 4k $\times$ 4k correlation matrices for further analysis using the RADWARE analysis package [25].

III. EXPERIMENTAL RESULTS

The data were analyzed by adopting the analysis procedure outlined in Ref. [26]. The results show the presence of previously unobserved levels in ^{213}Rn and α-decay branches to ^{209}At, which are discussed in the following sections.

A. ^{213}Rn

The ground state of ^{213}Fr decays 99.44(5)% of the time via α emission to ^{209}At while the remaining fraction [0.56(5)%] disintegrates via EC/β^+ decay to ^{213}Rn [13]. Nevertheless, such a small decay branch could be studied mainly due to a relatively high production cross section compared to other isobars and the pure beam of ^{213}Fr. The ground-state $I^\pi = 9/2^-$ of ^{213}Fr was measured using the atomic beam magnetic resonance technique by Ekström *et al.* [27] while the accepted half-life of 34.82(14) s is a weighted average of several measurements [13]. A more recent reference [28] has reported a high-precision measurement of the half-life yielding $T_{1/2} = 34.14(6)$, using the LIfeTime Experiment (LITE) at the Istituto Nazionale di Fisica Nucleare Laboratori Nazionali del Sud (INFN-LNS).

Although many high-spin states in ^{213}Rn were established using heavy-ion fusion-evaporation reactions [29–31], no information was available on the states populated in the EC/β^+ decay of ^{213}Fr prior to our study. The γ rays in ^{213}Rn were identified with the help of γ-γ coincidences, γ-ray–x-ray coincidences, x-ray–conversion-electron coincidences, half-lives, and conversion-electron spectroscopy. Figures 3(a) and 3(b) show radon x rays when gated on 704.3-keV γ rays and 605.9-keV conversion electrons, respectively; while Fig. 3(c)
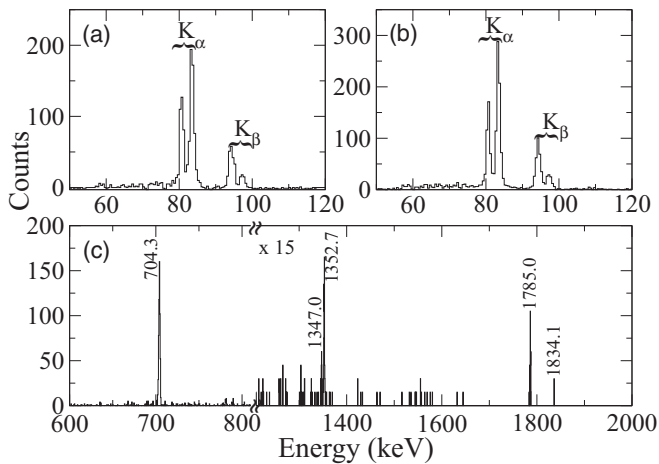
FIG. 3. Spectra showing radon K_α and K_β x rays obtained with gates on (a) 704.3-keV events from the γ-γ matrix and (b) 605.9-keV conversion electrons (corresponding to 704.3-keV γ rays) from a γ-ray$-$conversion-electron matrix. Panel (c) shows γ-ray spectra obtained from adding K_{α_1}, K_{α_2}, and K_{β_1} radon x-ray gates using the γ-γ matrix.

shows the γ-ray transitions observed in coincidence with radon x rays. Furthermore, the half-life obtained from the decay curve analysis of the 605.9-keV conversion electrons (corresponding to the 704.3-keV γ rays), as shown in Fig. 4, is consistent with the previous measurements [13,28] and helps to verify its origin. The observed transitions (see Table I) are from four new levels at 1347.0, 1352.7, 1785.0, and 1834.1 keV. Most of the observed levels are found to decay directly to the ^{213}Rn ground state. Only the 1785.0-keV level is found to decay in three different ways as shown in Fig. 5. Assuming that only allowed or first forbidden transitions can occur, all the levels mentioned above can have any spin from 7/2 to 11/2 with a possibility of either parity. This is not shown in Fig. 5 to keep the figure simple. The level at 704.3 keV decays
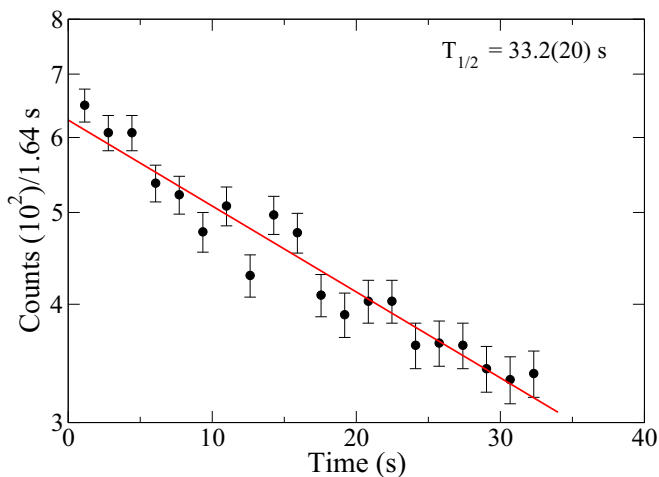

FIG. 4. Fit to the decay of the 605.9-keV conversion electrons corresponding to 704.3-keV γ rays in ^{213}Rn, which is populated in the EC/β^+ decay of ^{213}Fr.

via the 704.3-keV $M1$ transition (see Table I). Therefore, its spin-parity is identified as $11/2^+$. This level was reported at 705.0 keV in earlier studies [29–31].

Calculations of $\log ft$ values require knowledge of the decay intensities to each level. In the present experimental setup, however, it was not possible to determine the decay intensity to the ground state of the daughter nucleus. Therefore, the following method was used to estimate the minimum and maximum decay intensities to the ground state. It is known from the literature [13] that the ground state of ^{213}Fr decays to the ground state of ^{213}Rn via a first forbidden transition, for which the most probable $\log ft$ value is 7 [34]. This value requires 13% branching to the ^{213}Rn ground state. The $\log ft$ values of 6.6 and 7.4 require the decay to proceed with 30% and 5% of the actual decay intensity, viz., 0.56% to the ground state of ^{213}Rn, respectively. Further, assuming the above two values of ground-state branching, i.e., 30% and 5%, two values of the decay intensity were calculated for all the new levels. This, in turn, gives two different $\log ft$ values for each level. In Fig. 5, the average of the two $\log ft$ values is quoted for each level (with the exception of the ground state) and the uncertainty of the $\log ft$ values includes the uncertainty of the ground-state feeding.

The above approach is justified because the calculated $\log ft$ value of 6.05(11) for the decay to the first excited state in ^{213}Rn is in good agreement with that for the similar transitions in the neighboring nuclei [13]. Also, the lower limit of the $\log ft$ value to the ground-state decay is 6.1, i.e., with all β-decay intensity (0.56%) going to the ground state of ^{213}Rn.

B. ^{209}At

Although 99.44% of the ^{213}Fr decays occur by α emission to ^{209}At, only three α-decay branches were identified in a recent work by Kuusiniemi *et al.* [9]. Earlier studies [35–37] have observed only one α-decay branch, populating the ground state of ^{209}At. The ground state of ^{209}At is identified as $9/2^-$ based on the favored α decay to the $9/2^-$ ground state of ^{205}Bi [38]. High-spin states were established in experiments employing fusion-evaporation reactions [39–43]. In addition, several states with angular momenta ranging from 3/2 to 7/2 were observed in the electron-capture decay of the ground state of ^{209}Rn, which has $I^\pi = 5/2^-$ [44].

The three α-decay branches populate previously known [38] levels at 0.0, 408.3, and 577.0 keV. Among these, the ground-state to ground-state decay branch is observed to carry 99.78% of the total α-decay intensity [9]. Apart from confirming the decay to the 408.3- and 577.0-keV levels, we have identified new α-decay branches populating states reported earlier at 745.7, 789.0, 1081.2, 1097.7, and 2820.6 keV in ^{209}At [38]. The new branches were established on the basis of various coincidence relationships between the γ rays, x rays, and conversion electrons. Figure 6 illustrates summed spectra obtained with gates on the 408.3- and 689.4-keV γ rays. The intensities of all the transitions, except the 380.7- and 689.4-keV γ-ray transitions, were determined from the singles spectra. The 380.7- and 689.4-keV γ-ray transitions were not visible in the singles spectra. Therefore, their intensities were extracted using the spectra obtained with a gate on the

TABLE I. Table of γ-ray energies and relative intensities for transitions in ^{213}Rn. The measured K, L, and M conversion coefficients are given for the 704.3-keV transition together with the corresponding theoretical values [32] for $E1$, $E2$, and $M1$ multipolarities. The uncertainties in the energies are within 0.5 keV.

Transition energy (keV)	Relative intensity (I_γ)	Conversion shell	Experimental conversion coefficient (10^{-3})	Theoretical conversion coefficient			Assigned multipolarity
				$E1$ (10^{-3})	$E2$ (10^{-3})	$M1$ (10^{-3})	
438.0	2.6(3)						
704.3	100	K	50.2(59)	4.622	12.14	49.26	$M1$
		L	9.7(13)	0.7519	3.207	8.626	
		M	2.3(3)	0.1762	0.7946	2.040	
1080.7	3.1(5)						
1129.8	Weak						
1347.0	16.4(14)						
1352.7	22.7(19)						
1785.0	16.4(14)						
1834.1	4.3(5)						

408.3-keV transition. The large errors in the intensities of these transitions (see Table II) are due to low statistics in the gated spectra. The 855.4- and 867.5-keV transitions along with the 408.3- and 689.4-keV transitions form a 408.3-, 689.4-, 855.4-, 867.5-keV sequence of γ-ray transitions, thereby establishing the levels at 408.3, 1097.7, 1953.1, and 2820.6 keV. Although the 855.4- and 867.5-keV transitions are very weak in the coincidence spectra, it is evident (see Fig. 6) that they have

almost equal intensities. Therefore, the level at 1953.1 keV does not have direct α-decay feeding. The possibility that the abovementioned states in ^{209}At could also have been populated in ^{213}Ra α decay followed by the EC/β^+ decay of its daughter nucleus (^{209}Rn) can be discarded on the basis of decay-curve analysis that reflects the origin of the γ rays, because the ground states of ^{213}Fr and ^{209}Rn have very distinct half-lives, 34.14 s and 28.5 min, respectively. One such decay curve

FIG. 5. Level scheme of ^{213}Rn as obtained from the β decay of ^{213}Fr. All the transitions are labeled with their energies and relative γ-ray intensities in brackets. The numbers on the right indicate the excitation energy of each level in keV. The EC/β^+ branching ratio of ^{213}Fr and the ground-state half-life of ^{213}Rn are from Ref. [13]. The ground-state half-life and the EC/β^+-decay Q value of ^{213}Fr are from Refs. [28,33], respectively.
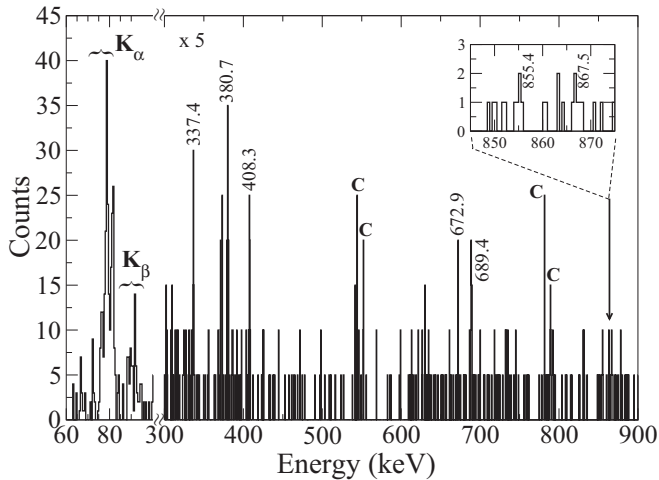
FIG. 6. The spectrum obtained from the sum of gates on the 408.3- and 689.4-keV γ-ray transitions in ^{209}At populated via α decay of ^{213}Fr. The inset illustrates the evidence of the 855.4- and 867.5-keV γ rays and the letter "C" denotes contaminant γ rays known from the decay of ^{209}At.

is shown in Fig. 7 for the 577.0-keV γ rays. The fit to the decay curve yields a half-life of 28.4(35) s, which is in reasonable agreement with that of the ground state of ^{213}Fr, thus supporting its origin from ^{213}Fr α decay.

However, as in the case of EC/β^+ decay, it was not possible to determine the ground-state to ground-state α-decay branching. Therefore, it was estimated using the data from Ref. [9] and intensities of γ transitions from the present work as explained below. The intensities of α particles that populate the ground state and the 408.3- and 577.0-keV levels are 99.78%, 0.12%, and 0.10% of the total α decay, respectively [9]. Further, the γ-ray intensities were used to determine the α-decay intensities to the excited states in ^{209}At. The ratio of the intensity of α particles that populate the excited state at 408.3 keV (0.12%) to that of the ground state (99.78%) was used as a normalization factor to estimate the branching to the ground state in the present study. The errors on the α

TABLE II. Table of level energies, relative α intensities, hindrance factors, γ-ray energies, and relative γ intensities in ^{209}At as observed in the α decay of ^{213}Fr. The uncertainties in the energies are within 0.5 keV.

E_{level} (keV)	Relative α intensity	Hindrance factor	E_γ (keV)	Relative γ intensity
0.0	99.72	2		
408.3	0.12	39	408.3	100
577.0	0.07	12	577.0	40.7(7)
745.7	0.04	4	337.4	6.8(5)
			745.7	14.1(6)
789.0	0.02	4	380.7	11.2(47)
1081.2	0.02		672.9	8.3(9)
1097.7	0.01		689.4	7.4(39)
1953.1			855.4	Weak
2820.6			867.5	Weak
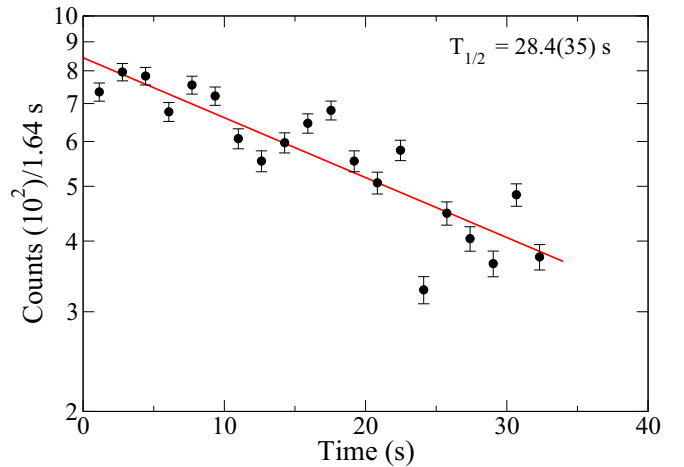
FIG. 7. Fit to the decay of the 577.0-keV γ ray in ^{209}At populated via α decay of ^{213}Fr.

intensities to the various levels are less than 15%, except for the levels at 789.0 and 1097.7 keV, for which the errors are close to 50% due to large errors in the intensities of associated γ-ray transitions (see Table II). The decay scheme derived from the above analysis is presented in Fig. 8. The α-decay hindrance factors were calculated using an approach described in Ref. [45].

IV. DISCUSSION

The spectroscopic study of nuclei, especially odd-A nuclei, in the vicinity of the heaviest stable doubly magic nucleus ^{208}Pb is a topic of great interest because they provide direct information on the underlying single-particle states. Some of the states that can be populated in β and α decay are otherwise inaccessible in in-beam γ-ray spectroscopy. In the following sections, we discuss the levels observed in the EC/β^+ and α decay of ^{213}Fr.

A. ^{213}Rn

^{213}Rn has one neutron outside the $N = 126$ shell closure. It has been well studied using heavy-ion fusion-evaporation reactions [29–31] and also in the context of its α decay [36]. However, as mentioned earlier, no states were known in ^{213}Rn following the EC/β^+ decay of ^{213}Fr prior to this work. High-spin studies have established several isomers in this $N = 127$ isotone, of which the majority decay via enhanced $E3$ transitions [29], which is a characteristic of the $N = 127$ isotones.

All the shell-model orbitals ($2g_{9/2}$, $1i_{11/2}$, $1j_{15/2}$, $3d_{5/2}$) available for the last odd neutron above the $N = 126$ shell gap have positive parity except $1j_{15/2}$. Therefore, the low-lying levels in ^{213}Rn are expected to have positive parity due to the coupling of the $2g_{9/2}$ and $1i_{11/2}$ orbitals to levels in the neighboring even-even nuclei. The ground state of ^{213}Rn was assigned the $\nu2g_{9/2}$ configuration by analogy with the ^{209}Pb and ^{211}Po isotones, and it was reported to α decay with 100% branch [13]. The first excited state was earlier reported to be at 705.0 keV with a tentative assignment of $11/2^+$ [29–31]. This state can be understood as a neutron excitation from $2g_{9/2}$
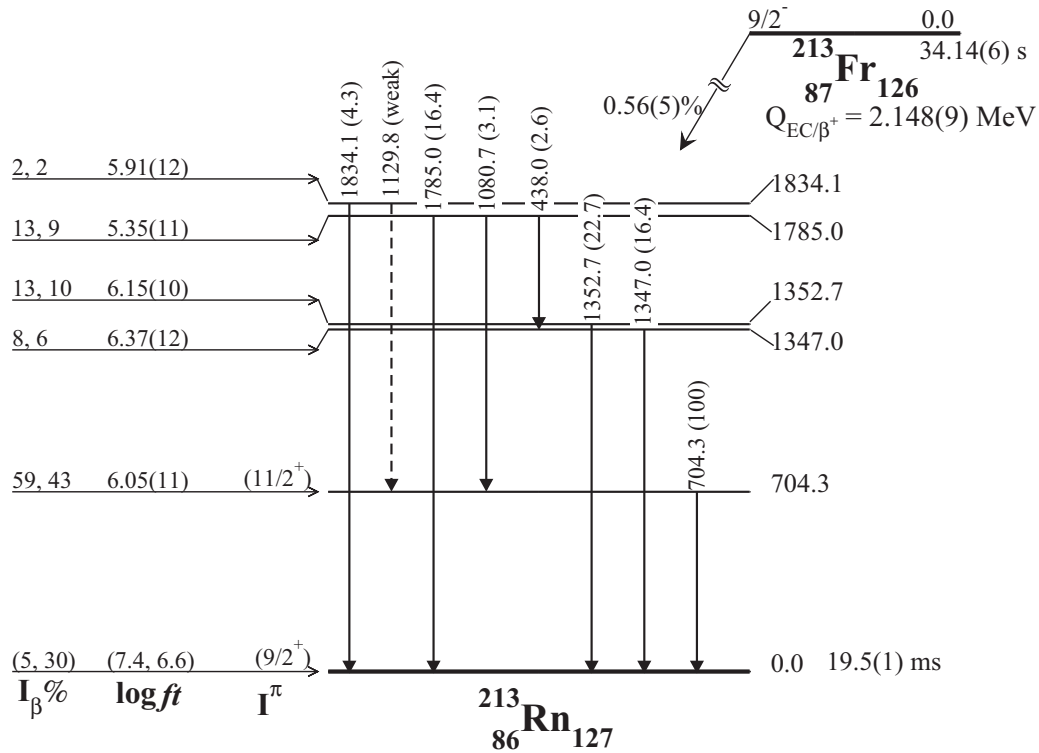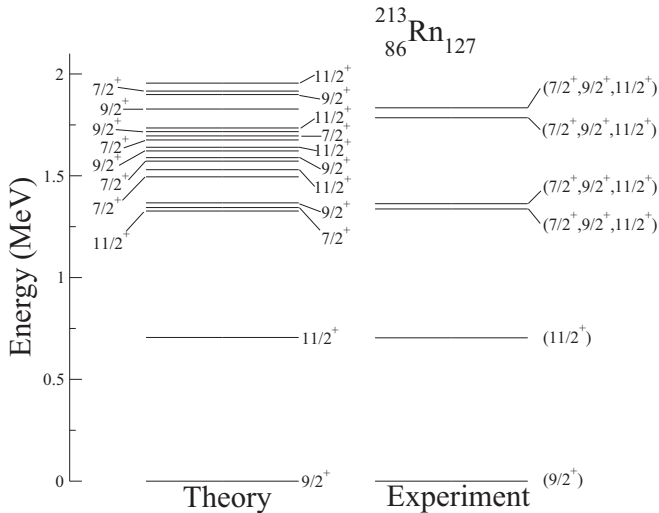
FIG. 8. Level scheme of ^{209}At as obtained from the α decay of ^{213}Fr. All the transitions are labeled with their energies. The numbers on the left side indicate the spin-parity, relative α-decay intensity, and hindrance factor; while those on the right side indicate the excitation energy of each level in keV. The spin-parity values and the ground-state half-life of ^{209}At are taken from Ref. [38]. The ground-state half-life and α-decay Q value of ^{213}Fr are from Refs. [28,33], respectively.

to $1i_{11/2}$. Both the states were observed in the present work. Apart from this, four new levels forming two groups around 1350 and 1800 keV were observed.

Shell-model calculations, using the OXBASH code [46] employing the KHP interaction [47], were performed to understand these new levels. The valence space consists of four protons in the $1h_{9/2}$, $2f_{7/2}$, $2f_{5/2}$, $3p_{3/2}$, $3p_{1/2}$, and $1i_{13/2}$ orbitals and a neutron in the $1i_{11/2}$, $2g_{9/2}$, $2g_{7/2}$, $3d_{5/2}$, $3d_{3/2}$, $4s_{1/2}$, and $1j_{15/2}$ orbitals. The calculations show that in the predominant configurations the protons are distributed among the $1h_{9/2}$, $2f_{7/2}$, and $1i_{13/2}$ orbitals; while the neutron remains in the $2g_{9/2}$ orbital, except for the first excited state where it occupies $1i_{11/2}$ as mentioned earlier. All the states below 2 MeV are predicted to have positive parity. The agreement between the experimental and the theoretical levels is excellent as shown in Fig. 9. Therefore, we can discard the possibility of negative parity for all the newly observed experimental levels. However, it is not possible to uniquely assign spins to each level in the two groups.

B. ^{209}At

There are nine known, $N = 126$ unstable isotones with $Z > 83$ [48]. All of them, except ^{211}At, are known to decay

via almost 100% α-emission populating states in the $N = 124$ isotones [4–12]. Further, these decays are observed to populate the ground states in their daughter nuclei with more than 99% of the total α-decay intensity. This could be understood as a favored α decay between the 0^+ ground state of the parent and daughter nuclei for even A. In the case of odd-A isotones, however, it is a consequence of the fact that the last unpaired proton, in both the parent and the daughter nuclei, occupies the $1h_{9/2}$ orbital. The weak decay branches were discovered by the α-γ coincidence technique, mainly at GSI, Darmstadt [5–9]. Among the $N = 126$ isotones, the most detailed α-decay data are available for ^{215}Ac with seven branches [7], including the ground-state branch. Similarly, along the odd-A francium isotopic chain, only ^{211}Fr and ^{213}Fr are known to have four and three α-decay branches, respectively [9]; while the remaining odd-A isotopes with $N < 126$ are observed to decay only to the ground state [35,37].

Recently, some effort has been made to provide a theoretical understanding of α decay in the vicinity of the $N = 126$ neutron shell closure [1,2]. These studies have evaluated α-preformation factors that contain nuclear structure information. Such studies are expected to help in investigations of superheavy nuclei and their structure. It is, therefore, essential to have precise and detailed experimental data on α decay

FIG. 9. Comparison of experimental and shell-model levels in ^{213}Rn.

in the $N = 126$ region. Fisichella *et al.* have significantly (few per mil) improved the precision with which the half-life of ^{213}Fr was measured prior to their work [28]. In the present work, we have significantly improved knowledge of the α-decay fine structure of ^{213}Fr. As mentioned in the last section, the hindrance factors were calculated using an approach outlined by Poenaru *et al.* [45] with a set of parameters suggested in Ref. [49]. The calculated hindrance factors are consistent with previous spin-parity assignments [38] and with the neighboring isotopes. The absence of the α-decay branch to the $7/2^+$ level at 1953.1 keV in ^{209}At is a consequence of the parity change between the initial state and the final state, and it is known that such α decays are more hindered than those in which parity remains the same [50]. The levels at 1081.2 and 2820.6 keV were assigned tentative spin with possible values of 5/2 or 7/2 from the electron capture studies of ^{209}Rn, which has

ground-state $I^\pi = 5/2^-$ [38]. Further, there is no evidence of population of the levels at 725.05 and 794.62 [38] keV in our study, for which ΔJ between the parent and the daughter is greater than 1. This might be an indication that the levels at 1081.2 and 2820.6 keV have 7/2 spin.

V. SUMMARY

In summary, we have performed for the first time EC/β^+ decay study of the $N = 126$ isotone, ^{213}Fr, at ISOLDE, CERN, with the help of γ-ray and conversion-electron spectroscopy. Several new γ rays have been identified that establish hitherto unknown excited states in ^{213}Rn. Also, five new α-decay branches from the ^{213}Fr ground state have been discovered based on the observed γ rays following the α decay. Shell-model calculations have been performed to understand the newly observed states in ^{213}Rn. The calculations are in excellent agreement with the experimental results for ^{213}Rn and allow us to constrain the parities of the experimental levels to be positive. The α-decay hindrance factors are consistent with previous spin-parity assignments and with the systematics of the neighboring nuclei. More decay studies with better statistics are desirable to establish and understand the low-spin states in this region.

[1] C. Xu and Z. Ren, Phys. Rev. C **76**, 027303 (2007).
[2] Y. Qian and Z. Ren, Nucl. Phys. A **852**, 82 (2011).
[3] B. Singh, D. Abriola, C. Baglin, V. Demetriou, T. Johnson, E. McCutchan, G. Mukherjee, S. Singh, A. Sonzogni, and J. Tuli, Nucl. Data Sheets **114**, 661 (2013), and references therein.
[4] A. P. Leppänen, J. Uusitalo, M. Leino, S. Eeckhaudt, T. Grahn, P. T. Greenlees, P. Jones, R. Julin, S. Juutinen, H. Kettunen, P. Kuusiniemi, P. Nieminen, J. Pakarinen, P. Rahkila, C. Scholey, and G. Sletten, Phys. Rev. C **75**, 054307 (2007).
[5] F. P. Heßberger *et al.*, Eur. Phys. J. A **15**, 335 (2002).
[6] P. Kuusiniemi, F. P. Heßberger, D. Ackermann, S. Hofmann, B. Sulignano, I. Kojouharov, and R. Mann, Eur. Phys. J. A **25**, 397 (2005).
[7] P. Kuusiniemi, F. P. Heßberger, D. Ackermann, S. Hofmann, and I. Kojouharov, Eur. Phys. J. A **22**, 429 (2004).
[8] P. Kuusiniemi, F. P. Heßberger, D. Ackermann, S. Antalic, S. Hofmann, K. Nishio, B. Sulignano, I. Kojouharov, and R. Mann, Eur. Phys. J. A **30**, 551 (2006).

[9] P. Kuusiniemi, F. P. Heßberger, D. Ackermann, S. Hofmann, and I. Kojouharov, Eur. Phys. J. A **23**, 417 (2005).
[10] M. J. Martin, Nucl. Data Sheets **108**, 1583 (2007), and references therein.
[11] F. G. Kondev and S. Lalkovski, Nucl. Data Sheets **112**, 707 (2011), and references therein.
[12] F. G. Kondev, Nucl. Data Sheets **109**, 1527 (2008), and references therein.
[13] M. S. Basunia, Nucl. Data Sheets **108**, 633 (2007).
[14] S. Hofmann and G. Münzenberg, Rev. Mod. Phys. **72**, 733 (2000).
[15] Yu. Ts. Oganessian *et al.*, Nature (London) **400**, 242 (1999).
[16] D. Seweryniak, K. Starosta, C. N. Davids, S. Gros, A. A. Hecht, N. Hoteling, T. L. Khoo, K. Lagergren, G. Lotay, D. Peterson, A. Robinson, C. Vaman, W. B. Walters, P. J. Woods, and S. Zhu, Phys. Rev. C **73**, 061301 (2006).
[17] B. Hadinia *et al.*, Phys. Rev. C **70**, 064314 (2004).
[18] C. Nociforo *et al.*, Phys. Scr., T **150**, 014028 (2012).

[19] J. Zhang, M. Tandecki, R. Collister, S. Aubin, J. A. Behr, E. Gomez, G. Gwinner, L. A. Orozco, M. R. Pearson, and G. D. Sprouse, Phys. Rev. Lett. **115**, 042501 (2015).

[20] J. Crawford, P. Schaffer, and T. Ruth, J. Nucl. Med. **55**, 1414 (2014).

[21] U. Köster (ISOLDE Collaboration), Radiochimica Acta **89**, 749 (2009).

[22] R. Barden, Ph.D. thesis, Johannes-Gutenberg Universitaet Mainz, 1988.

[23] A. B. Pérez-Cerdán *et al.*, Phys. Rev. C **84**, 054311 (2011).

[24] http://www.xia.com/DGF_Pixie-4.html.

[25] D. C. Radford, Nucl. Instrum. Methods Phys. Res., Sect. A **361**, 297 (1995).

[26] A. Y. Deo, Zs. Podolyák, P. M. Walker, A. Algora, B. Rubio, J. Agramunt, L. M. Fraile, N. Al-Dahan, N. Alkhomashi, J. A. Briz, E. Estevez, G. Farrelly, W. Gelletly, A. Herlert, U. Köster, A. Maira, and S. Singla, Phys. Rev. C **81**, 024322 (2010).

[27] C. Ekström, S. Ingelman, G. Wannberg, and M. Skarestad, Phys. Scr. **18**, 51 (1978).

[28] M. Fisichella, A. Musumarra, F. Farinon, C. Nociforo, A. Del Zoppo, P. Figuera, M. La Cognata, M. G. Pellegriti, V. Scuderi, D. Torresi, and E. Strano, Phys. Rev. C **88**, 011303(R) (2013).

[29] A. E. Stuchbery, G. D. Dracoulis, A. P. Byrne, S. J. Poletti, and A. R. Poletti, Nucl. Phys. A **482**, 692 (1988).

[30] Y. Fukuchi, T. Komatsubara, H. Sakamoto, T. Aoki, and K. Furuno, J. Phys. Soc. Jpn. **57**, 2976 (1988).

[31] T. Lonnroth, C. W. Beausang, D. B. Fossan, L. Hildingsson, W. F. Piel, Jr., and E. K. Warburton, Phys. Scr. **39**, 56 (1989).

[32] T. Kibédi, T. W. Burrows, M. B. Trzhaskovskaya, P. M. Davidson, and C. W. Nestor, Jr., Nucl. Instrum. Methods Phys. Res., Sect. A **589**, 202 (2008).

[33] G. Audi, A. H. Wapstra, and C. Thibault, Nucl. Phys. A **729**, 337 (2003).

[34] B. Singh, J. L. Rodriguez, S. S. M. Wong, and J. K. Tuli, Nucl. Data Sheets **84**, 487 (1998), and references therein.

[35] R. D. Griffioen and R. D. Macfarlane, Phys. Rev. **133**, B1373 (1964).

[36] K. Valli, E. K. Hyde, and W. Treytl, J. Inorg. Nucl. Chem. **29**, 2503 (1967).

[37] P. Hornshøj, P. G. Hansen, and B. Jonson, Nucl. Phys. A **230**, 380 (1974).

[38] J. Chen and F. G. Kondev, Nucl. Data Sheets **126**, 373 (2015), and references therein.

[39] D. Dracoulis, C. A. Steed, A. P. Byrne, S. J. Poletti, A. E. Stuchbery, and R. A. Bark, Nucl. Phys. A **462**, 576 (1987).

[40] T. P. Sjoreen, G. Schatz, S. K. Bhattacherjee, B. A. Brown, D. B. Fossan, and P. M. S. Lesser, Phys. Rev. C **14**, 1023 (1976).

[41] V. Rahkonen and T. Lonnroth, Z. Phys. A **322**, 333 (1985).

[42] I. Bergstrom, C. J. Herrlander, T. Lindblad, V. Rahkonen, K.-G. Rensfelt, and K. Westberg, Z. Phys. A **273**, 291 (1975).

[43] P. Mukherjee, P. Sen, I. Mukherjee, and C. Samanta, J. Phys. G **16**, L107 (1990).

[44] B. Jonson, M. Alpsten, A. Appelqvist, B. Bengtsson, and K. A. Johansson, Phys. Scr. **8**, 142 (1973).

[45] D. N. Poenaru, M. Ivascu, and D. Mazilu, J. Phys. Lett. **41**, 589 (1980).

[46] B. A. Brown, A. Etchegoyen, W. D. M. Rae, N. S. Godwin, W. A. Richter, C. H. Zimmerman, W. E. Ormand, and J. S. Winfield, MSU-NSCL Report No. 524, 1985.

[47] E. K. Warburton and B. A. Brown, Phys. Rev. C **43**, 602 (1991).

[48] E. Caurier, M. Rejmund, and H. Grawe, Phys. Rev. C **67**, 054310 (2003), and references therein.

[49] E. Rurarz, Acta Phys. Pol., B **14**, 917 (1984).

[50] M. Asai, F. P. Heßberger, and A. Lopez-Martens, Nucl. Phys. A **944**, 308 (2015), and references therein.